Response to Referee #2
Warm protons at comet 67P/Churyumov-Gerasimenko – Implications for the infant bow shock

We thank the referee for the constructive comments and suggestions. We have made the necessary amendments to the paper and answers to comments may be found below. (Blue: Referee comment, black: our answer).

The principal diagnostic is the observation of 'warmer, slower' protons, but this is not quantified in the paper as much as it could be, although visible in spectrograms. Some simple 1D analysis (building on the vm,H shown here) would allow calculation of the velocity, but the main suggestion here is that at least some analysis and characterisation of the width of the proton spectra, and the jump across the feature, would provide a quantitative indication related to temperature, which is missing from the current analysis although it is a prime diagnostic.
Line 64 – 'proton velocity distribution becomes broader and the bulk velocity decreases' – visible in the spectrograms usually, but needs some quantification (see comment 1 above)
Line 200-215 – the authors could usefully define and calculate a parameter associated with the width of the proton distributions (as with the velocity change vm,H this is a key indicator) – see also comment 1 above Section 3.3 general comment – is there any evidence for larger/more developed jumps with increasing Q?
Line 238 – 'protons with higher temperatures' - this should be quantified, see comment 1
Indeed, it would be good to look at the width/temperature of the protons as well as the spectra. We have used a temperature dataset, derived from the proton spectra, when initially selecting intervals. However, it turned out to be not very useful, because the correctness of the temperature depends on there being no cross-talk between mass channels in the ICA instrument as well as a good signal to noise ratio. Crosstalk is a well known issue and not easy to correct for, especially in an automatically generated data set. The attached figure shows the events from Figure 1 and 6 in the paper, with the temperature added. While the temperature describes the proton signature in the spectra very well for the event in July 2016, is does not do so for February 2016. In the ICA solar wind spectra, it becomes clear that there is significant cross-talk where signatures from cometary ions appear in the solar wind spectra. Thus we discarded this parameter for further statistical analysis. However, since the temperature dataset is suitable for a more thorough investigation of a smaller set of events, we have included the temperature in all figures and now discuss it in Sect. 3.1.

Some calculations of Mach number based on the analysis of Smith et al (1986) for comet GZ and Coates et al (1990, 1997) could be attempted for at least some of the observed 'infant bow shock' features in the data, as well as in the related simulations. This would strengthen the use of the word 'shock', and allow comparison to 'shocklets' seen in other simulations (e.g. Omidi et al). The change in velocity, magnetic field and density could be estimated sufficiently to do this.
Line 310 – Kessel et al (JGR, 1994) also reformulated the jump conditions and determined shock normal for multiple ion shocks
In the discussion, we touch very briefly on this point, but we see that this could be further elaborated. The assumptions made by Coates et al (1990) for the discussion of the shock are: low cometary ion density fraction (1.5%), single fluid 1D model with a mass source term in the continuity equation, a steady state. None of these apply for the case of 67P. At 67P at this stage the cometary ions dominate density wise and are as important as the solar wind momentum wise. They constitute not only a mass source, but also a momentum source (Nilsson et al 2020). The 1D approximation does not hold, because significant deflection of the solar wind and cometary ions has already happened by the time the solar wind reaches the region where Rosetta is located (see e.g. Behar et al 2016). As Rosetta can only observe a boundary when the boundary itself is moving, everything we observe is inherently not in a steady state.

Thus, the model used by Coates et al (1990) is not applicable here. The solution presented by Kessel et al (1994) does include the second ion population, but otherwise suffers from the same problems. Instead we looked at two-ion shocks that treat ions as particles and not fluids. The most applicable example is that of Fahr & Siewert (2015). As detailed in the text, we cannot get a good estimate of the proton density alone and thus it is not possible to actually test the model by Fahr & Siewert for this case.

In Figure 3, some of the vm,H values indicate an increase of velocity from upstream to downstream – this seems counter-intuitive for any shock

This is true. As discussed for the temperature above, and in the text for $v_{m,H}$, this parameter is not very well suited for usage in a statistical study. It needs to be treated with caution, which we have done for the smaller subset of events, but chose not to do for the large dataset. A reexamination of the parameter has reaffirmed this. To avoid confusion, this parameter was removed from figure 3 and is only discussed in the text now.

Line 23 – the text refers to a 'fully formed shock' at comets, but has this been observed by Rosetta? The references provided all relate to Rosetta. Additional references include Smith et al, 1986, Coates et al, 1990, 1996, relating to GZ, Halley and GS.Line 28 – Mass loading, deceleration and deflection were all aspects of earlier studies on Giotto and AMPTE data which are not referenced here (Coates et al., 2015, and references therein, are relevant)Line 38 – the convective electric field upstream of the comet drives the pickup process as shown in earlier studies (e.g. Neugebauer et al., 1989, Coates et al., 1990 and many other studiesLine 45 – the bow shock location, formation and features have been studied in detail using data from Giotto by others also (e.g. Coates et al., 1990, 1996)Lines 54-55 – Bow shock studies at comets and other solar system objects have been more extensive than the references would indicateLine 69 – please specify the 'similarity to a bow shock at a fully developed comet', using references from earlier missions – which changes were seen before and which are different here

We focused here more on the observations at 67P, but indeed a more extensive summary also of observations at other comets is beneficial. This was added.

Line 66 typo 'ensure'

Corrected

Line 83 – 'Often, the signal is still visible in the RPC-IES instrument' – presumably due to different FOV, please add a comment .

Yes, this is due to FoV effects. A comment was added.

Line 93 – 'partially complementary to ICA' – please specify the fields of view and extent of overlap/complementarity

The field of view is partially complementary. The exact FoV can be found in the ICA User Guide, available on the PSA. We have added a reference to this in the text.

Line 115 – 'need to be at significantly lower energies' – please quantify

The peak of the proton energy distribution needs to decrease by at least 60eV (corresponding to three ICA energy bins, at the lowest proton energies (250 eV)). This was added in the text.

Line 157 – It is interesting that the alpha particle and He+ spectra follow the proton distributions yet both remain distinct, another indication that the transitions are weak, a comment could be added on this

This is a good point, it was added.

Line 163 – More precise to say 'is more negative' rather than 'lower'

Agreed.

Line 164-5 – 'the lower the spacecraft potential, the higher the density' could be reworded 'higher plasma density would increase the flux of electrons to the spacecraft, providing more negative spacecraft potentials'

Since the calibrated density is now available, we have substituted the spacecraft potential by the actual density. This changes nothing in terms of the discussion and conclusions.

Line 165 – 'This the density is higher' – how much higher, and where? How is this visible in the data shown? Fig 2 caption – add comment (see definitions in text), or add a short explanation for the definition of the parameters shown

Previously this was not visible in the data, as we could not show the density. Since we have now included the density instead of the spacecraft potential this should be taken care off. Fig. 2 caption was expanded to be more self-explanatory.

Line 178 – 'transition can sometimes be very broad' – can this be quantified e.g. with respect to the electron, proton and heavy ion gyroradius? (see e.g. Coates et al. 1990)

I think it is not clear how we can relate this transition time to a scale. We do not know the velocity of the boundary and we dare not make assumptions.

Line 190 typo 'where'

Corrected

Line 224 – as well as Deca et al, there were earlier papers on momentum balance in the AMPTE releases and in comets (see Coates et al. 2015, and references therein, eg Coates et al, JGR 1986, Johnstone et al., Geophys. Monograph 38, 1985, Coates et al, Adv Space Res 1988))

The Deca et al paper gives a particularly good example of the deflection at a comet with details on the different behaviour of all particle species (solar wind electrons, ions, cometary electrons, ions). This kind of deflection is not explicitly addressed in models based on a fluid approach. We have added Coates et al. 2015 as a reference for observations of deflection at 67P.

Line 242 – 'flux of electrons does increase downstream' – might some of this be associated with spacecraft potential changes?

This is unlikely, we corrected for the spacecraft potential effect in the spectra shown here (see section 2.1). For the energies that we are looking at here (60eV and over) the spacecraft potential has very little effect on the measured energy spectra.

Line 250 - 'different for electrons and protons' – and heavy ions?

Indeed. This was added in the text.

Line 254 – Might shocklets (e.g. Omidi et al.), and/or upstream cavities, be relevant

Omidi et al. 1984 conducted one-dimensional hybrid simulations with the aim of modelling the spacecraft encounters with comets 1P/Halley and 21P/Giacobini-Zinner. They found that for oblique interaction (cone angle 55°), shocklets form in a region of large amplitude wave activity. These shocklets convect downstream, where they break up due to dispersion, and new ones form further upstream. Thus, the process is repeated in a way that resembles shock reformation at planets (Balogh et al 2013). Although it is possible that shocklets form and shock reformation occurs also at comet 67P under certain conditions, it is not the cause of the observations reported here. The shock encounters shown in the paper do not display the repetitive transitions in a wave-dominated region that would be expected for the shocklets reported by Omidi et al. This discussion was added to the text at the end of section 4.

Line 262 – 10s of minutes – how might this compare to gyroperiods/radii?

The gyrofrequency of a proton in a 20nT field is $2s^{-1}$, for water ions it is $0.1s^{-1}$. Thus, we are well above the gyroperiod scales. In fact, all transition times that we observe are longer than the gyro period.

Line 274 – please specify/clarify/indicate on Fig 6 the times discussed (first/second half)

The term first and second half refer to the times with and without ICA observations. As the missing data is quite clear in the figure we do not think it is necessary to mark it, however, the text was rephrased to make it clear that we refer to the time with/without ICA spectra.

Line 283 – 'density of the plasma does not change significantly' – if anything, the spacecraft potential is more negative, thus density higher, in the 'upstream' region in this case

This statement seems to have been unclear. This sentence was supposed to refer to the average

behaviour, not the specific event shown in Figure 6. This was clarified in the text, and we have also pointed out that events with increased, decreased, and unchanged density can all be found.

Line 285 – could calculate the ratio between the solar wind and the local plasma density

Indeed, this is a good point. We cannot do this for all events due to data quality of the proton moments, but we did take a look at the event from Figure 1 and found a proton density of ca $0.5\,\mathrm{cm}^{-3}$ for this event. The plasma density is of the order of $1000\,\mathrm{cm}^{-3}$, this would mean a proton fraction of 0.05%. This seems rather low, however, the proton density estimate is also extremely low. Even assuming that ICA underestimate by a factor of 10, would only give us a fraction of 0.5%. Thus, for the larger plasma dynamics, the protons can be neglected. Alternatively we can make an estimate of the maximum proton density based on a simple fluid model, which seems a better way to get the maximum fraction of protons in the plasma. We have added to the paper: " We can estimate the fraction of cometary ions for the event shown in Fig. 1. The cometary ion density is of the order of $1000\,\mathrm{cm}^{-3}$ and we can estimate the maximum proton density from a simple back-of-the-envelope calculation: assuming a solar wind density of $3\,\mathrm{cm}^{-3}$ (typical for heliocentric distances around 2 AU) and a compression factor of ~ 4, we get a proton density of $12\,\mathrm{cm}^{-3}$. This is close to what is also observed in the simulation used below. This gives a fraction of $\sim 99\%$ cometary ions. Even if this estimate is very rough, it is clear that the cometary ions are at this point clearly dominating the plasma and the solar wind has only very little influence on the plasma density."

Line 288 – it would be useful to mention the assumed gas production rate Q in simulation and for the relevant observation

The gas production rate for the simulation was $3.2 \times 10^{27}\,\mathrm{s}^{-1}$. We added this to the text.

Line 290 – please indicate the suggested 'IBS' location on Fig. 5

A description was added in the caption.

Line 294 – what is the scale of proton gyration compared to the features seen in the simulation

The gyroradii of protons in the $200 - 400\,\mathrm{km\,s}^{-1}$ range are $100 - 200\,\mathrm{km}$ in a $20\,\mathrm{nT}$ magnetic field. This is comparable to the thickness of the infant bow shock. The typical length scale of the structure in the upper left corner of Fig. 5 is about $10^3\,\mathrm{km}$, corresponding to approximately 2 gyroradii in the weaker magnetic field ($\sim 10\,\mathrm{nT}$) in that region. This was added in the text.

Line 299 – Does +Ec correspond to Eparallelz as on the Figure?

Indeed, a clarification was added to the caption of the figure.

Line 306 – 'not significant enough to form a large bow shock' – rather than 'large' do you mean fully developed? Might there be a relation to shocklets?

On shocklets, see comment above. Yes, *fully developed* is a better descriptor, this was changed.

Line 322 – Re shock motion – as mentioned above, it should be possible to estimate the shock motion speed from the change in velocity and shock normal (e.g. Smith et al, Coates et al)

In general the normal is not well known, since knowing it would require measurements on both sides for the same conditions, and we generally only have slow transitions, where the conditions are likely to change.

Line 325 – please briefly explain the term 'caustic' Line 334 – re Comet Interceptor, depending on the gas production rate of the target comet, any observed cometary bow shock may be more fully developed than the features discussed here

Caustic is the term used in the referenced paper. A half-sentence describing it in more detail was added. Re Comet Interceptor, since the gas production rate of the comet to be visited is unknown, it is entirely possible to encounter an infant bow shock or a fully developed bow shock. We added an appropriate modifier in the text.

Line 340 – also, 3D fully kinetic simulations would be valuable

Indeed. This was clarified.

Line 345 – refers to a 'density proxy' – is this the spacecraft potential? In Fig 6 the density appears higher upstream

Since we now include the density, this is solved.

Line 355 – More accurate to say 'It may be that the 'infant bow shock' is the low production rate manifestation of what becomes the more developed cometary bow shock as observed at larger comets such as Halley' (add references). Also discuss shocklets in this context

This was reformulated. Shocklets are discussed in more detail in the previous section and since they are unrelated to the IBS we don't think a discussion of this belongs in the conclusion.

Line 357 – 'ordinary' may not be the correct adjective for the complex bow shock structure, with changes at proton and heavy ion gyroscales, as observed at comets such as Halley (e.g. Coates et al., 1987).

True. This was solved by adjusting the sentence above.

Significant Text Changes

~~Multiple plasma boundaries have been observed at~~ The plasma around comet 67P/Churyumov-Gerasimenko ~~.~~ ~~Among them was an~~ shows remarkable variability throughout the entire Rosetta mission. Plasma boundaries such as the diamagnetic cavity, solar wind ion cavity and infant bow shock ~~, an asymmetric structure~~ separate regions with distinct plasma parameters from each other. Here, we focus on a particular feature in the plasma~~environment that separates the less disturbed solar wind from a plasma with warmer, slower protons. Rosetta crossings of the infant bow shock have so far only been reported for two days. Here, we aim to investigate this phenomenon~~ : warm, slow solar wind protons. We investigate this particular proton population further by focusing on the proton behaviour and surveying all of the Rosetta comet phase data. We find over 300 events ~~that match the proton signatures at the infant bow shock~~where Rosetta transitted from a region with fast, cold protons into a region with warm, slow protons.

~~Both~~ These results agree well with simulations of the infant bow shock (IBS), an asymmetric structure in the plasma environment previously detected on only two days during the comet phase. The properties of the plasma on both sides of this structure

As a comet approaches the Sun, energy input into the surface increases ~~and with it~~ which increases the amount of ice that is sublimated and escapes into space.

At higher gas production rates this asymmetry is less pronounced and the influence of the cometary ion gyroradius is diminished, because the magnetic field pile-up at the comet results in higher field magnitudes and thus ~~lower gyroradii.~~ smaller gyroradii.

Boundaries in the plasma at 67P have been identified and characterized in many publications. The three main boundaries that were observable by Rosetta were, in order of decreasing cometocentric distance, the solar wind ion cavity (e.g. Nilsson et al., 2017), a collisionopause (Mandt et al., 2016), and the diamagnetic cavity (e.g. Goetz et al., 2016a,b). The solar wind ion cavity is the region where no solar wind ions can be observed in the plasma, from May 2015 to January 2016 Rosetta was almost exclusively within this region. The collisionopause demarcates the tenuous boundary where ion-neutral or electron-neutral collisions become important and it has been shown to lie within the solar wind ion cavity. Finally the diamagnetic cavity is the innermost observed region, where the magnetic field is very close to zero. For a more detailed overview of these boundaries see e.g. Götz et al. (2019).

Another boundary in the plasma environment of a comet, but not observed by Rosetta, is the bow shock.

There, the interaction between the solar wind and the comet cannot be described by mass-loading alone, instead the flow changes from supersonic to subsonic and a bow shock forms. This prediction is shown to fit well with observations at e. g. comet Halley (Neubauer et al., 1986), where the bow shock was detected 1.15×10^6 km from the nucleus. The transition from unshocked to shocked solar wind was identified by a decrease in speed, increase in density and temperature and an increase in the magnetic field (Coates et al., 1990). The shock was identified as a low Mach number shock, in agreement with the model, which predicted a gradual slowing of the solar wind flow already upstream of the shock due to the incorporation of the cometary ions. The cometary ion density is often neglected in bow shock models at high activity comets, because it only reaches 1.5-2.5% of the total density. Observations of bow shocks at other comets where quite similar, although at the lower activity comets Giacobini-Zinner (GZ) and Grigg-Skjellerup (GS) the bow shock is often termed a bow wave, due to the lack of a sharp boundary (Smith et al., 1986). At GS, a strong non-gyrotropy of the cometary ions could be observed near the bow wave, together with wave activity triggered by this unstable distribution function (Coates et al., 1996). Koenders et al. (2013) compare the bow shock distances from a simple single-fluid model with distances gained from Hybrid simulations and find that the fluid models predicted consistently higher stand off distances. Thus, the ion gyroradius effects are pronounced even in the most fluid-like stage of the plasma around comet 67P. ~~The shock~~

The shock itself forms by waves steepening into the nonlinear regime. The speed of the steepened wave is faster than that of the linear wave, but steepening is counteracted by dissipation. If an obstacle and a plasma are in relative motion faster than the speed of linear waves, the waves steepen until an equilibrium is reached where the shock becomes a stationary wave in the obstacle~~, in this case~~ 's (the comet's~~,~~) frame of reference (Balogh and Treumann, 2013).

~~Koenders et al. (2013) compare the bow shock distances from a simple single-fluid model with distances gained from Hybrid simulations and find that the fluid models predicted consistently higher stand off distances. Thus, the ion gyroradius effects are pronounced even in the most fluid-like stage of the plasma around comet 67P.~~

DIFaddbegin According to Balogh and Treumann (2013) , the slowing down and heating of the medium over a narrow layer or boundary is the defining feature of any shock.

Often, the signal is then still visible in the RPC-IES instrument, as the FOV is partially complimentary (rotated by 60°), a detailed description of the FoV can be found in the ICA User Guide on the PSA[1]. Solar wind

[1] https://cosmos.esa.int/web/psa/rosetta

Start time	H^+ E/q	$\Gamma_{IES,e}$	B_m	P_B	$\cos(\theta)$	~~$V_{s/c}$~~ n_{pl}	T_p	H^+ E/q	$\Gamma_{IES,e}$	B_m	P_B	$\cos(\theta)$	~~$V_{s/c}$~~
Dec 07, 14 03:49	↓	↑	–	↓	–	–	↑	↑	–	–	–	–	
Dec 25, 14 09:50	↓	↑	↓	↓	–		↑	↑	↓	–	–	–	
Jan 04, 15 12:19	↓	↑	–	↓	–		↑	↑	–	–	↑	–	
Jan 04, 15 19:55	↓	↑	↑	–	–		–	↑	↓	↑	–	↓	
Mar 07, 15 05:48	↓	↑	↑	↑	↑		↓	↑	↓	↓	–	↓	
Feb 10, 16 09:02								↑	↓	↓	↓	↓	
Feb 26, 16 05:50	↓	–	–	–	–	–	–	↑	–	↓	–	↓	
Feb 29, 16 00:27	↓	–	–	–	↓	–	–	↑	↓	↓	↓	↑	
Apr 08, 16 03:27	↓	↑	↓	↓	↑	↑		↑	↓	↑	↑	↓	
Apr 08, 16 07:58	↓	↑	↓	↑	–	↑	–	↑	↓	↑	–	↓	
Jun 01, 16 12:11	↓	↑	↑	↑	↑	–↑	↑						
Jul 09, 16 12:43	↓	↑	↑	↑	–	↑	↑	↑	↓	–	–	↓	
Jul 09, 16 15:52	↓	↑	↓	↓	–	↑	↑	↑	↓	–	–	↑	
Median	↓	↑	–	–	–	–↑	↑	↑	↓	–	–	↓	

Table 1: List of 13 events chosen for a more detailed study and list of parameter changes when crossing from upstream to downstream (inward, left) and from downstream to upstream (outward, right). The last line summarizes events by giving a median change. Missing signs indicate that no data was available.

densities near the comet also decrease due to significant charge exchange losses (Simon Wedlund et al., 2019). This caused rather low densities in the times when Rosetta was just outside the solar wind ion cavity. The RPC-ICA ~~moments~~ solar wind moments, including the temperature, used in this study are integrations of the RPC-ICA PSA L4 PHYS-MASS data set, also delivered to the planetary science archive (PSA) as RPC-ICA L5 MOMENT data set. ~~We chose to use the mean proton speed $v_{m,H}$ derived from this data set for assessment of the speed near the IBS. This value is derived by calculating the mean velocity of the proton energy distribution and thus is a more suitable parameter than the 3D velocity moment which is heavily influenced by the pitch angle distribution of the protons (Behar et al., 2017). Here, we only use values for which the density of the protons (calculated from the flux) is above 0.005 cm^{-3} which is the case for about 90% of all values.~~

~~Its FoV is partially complementary to ICA, but the~~ The time resolution is at least 256 s. ~~The~~, and the measurements at low energies are disturbed by the spacecraft potential, which is between 0 V and −20 V most of the time.

~~–~~(Johansson et al., 2020). For this study, we use the density estimate to characterize the plasma.

~~These are the two criteria used~~ For the first criterion, the threshold was a shift of the peak of the ion spectra by at least three energy bins, corresponding to at least 60 eV. We only use these two criteria for detection. For verification we evaluate additional properties like the ICA derived proton temperature, plasma density, suprathermal electron fluxes, magnetic field magnitude power spectral density in the frequency range between 50 mHz and 75 mHz and the magnetic field magnitude. However, the direction of change (increase or decrease) is not considered, ~~instead~~ because the change in parameters is simply an indicator that the change in proton energy and flux is not due to instrumental or spacecraft effects.

We also use the sun aspect angles of the spacecraft to exclude an attitude change of the spacecraft as a reason for a change in the proton signal. These are defined as the angles of the three spacecraft axes to the Sun-comet line[2]. Events that coincide with major attitude changes ($> 10°$) are not included in the study.

Other parameter changes like solar wind velocity and density as well as cometary ion density can also ~~cause~~ move the boundary, causing warm protons to appear ~~(as stated in previous publications)~~at the spacecraft (as stated in Gunell et al., 2018).

The He^+ and He^{2+} show a very similar behaviour to the protons (panel a), decreasing and broadening in energy, but their signature remains distinct from each other at all times. The IES electron signature (panel d) increases in energy and flux. Interestingly, the flux diminishes at the same time that the proton energy increases gradually~~.~~, implying that the spacecraft moved slowly upstream in a shock-fixed frame of reference into a region with less electron heating and a less slowed-down proton distribution. This is similar to what was observed already by Gunell et al. (2018).

This is because θ represents the angle between the x-axis and ~~magnetic~~ electric field, thus it does not reflect changes in the z-component of the magnetic field very well. The ~~spacecraft potential~~ plasma density (panel h) ~~is lower in the downstream region. We use this as a proxy for the density of the plasma: the lower the spacecraft potential, the higher the density. Thus the density is higher in the downstream region. We also ensure that these changes in the particle signatures are not due to a change in FoV, thus we included the spacecraft attitude~~ as well as the proton temperature (panel i) ~~to confirm that it only changes insignificantly in the time interval~~

[2]See `https://www.cosmos.esa.int/web/spice/spice-for-rosetta`

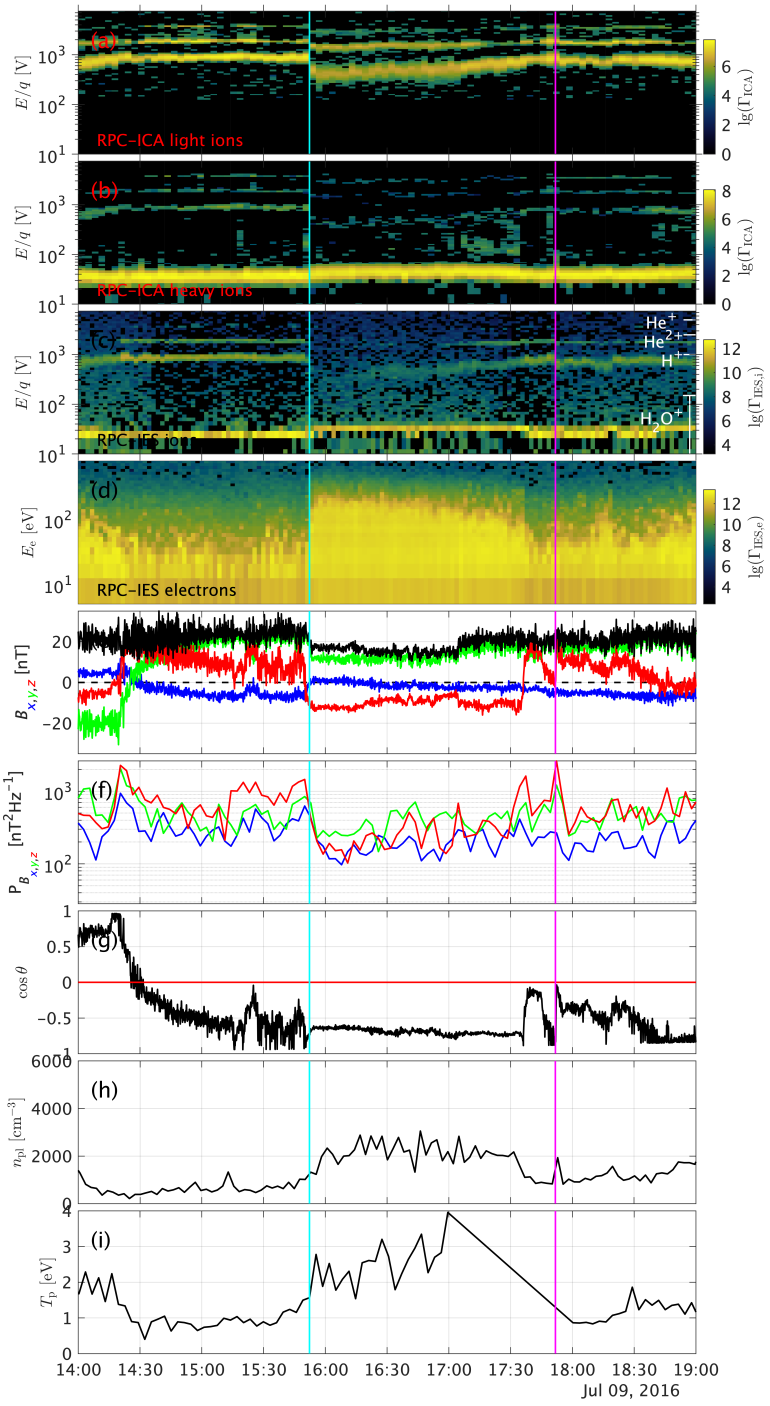

Figure 1: Observations of the event on July 9th, 2016. From top to bottom: a) ICA solar wind ions, b) ICA heavy ions, c) IES ions, d) IES electrons, e) magnetic field in CSEQ coordinates, f) magnetic power spectral density in the frequency range between 2 mHz and 15 mHz, g) angle between spacecraft position and convective electric field, h) ~~spacecraft potential~~plasma density from LAP, and i) ~~attitude~~1D proton temperature from ICA.

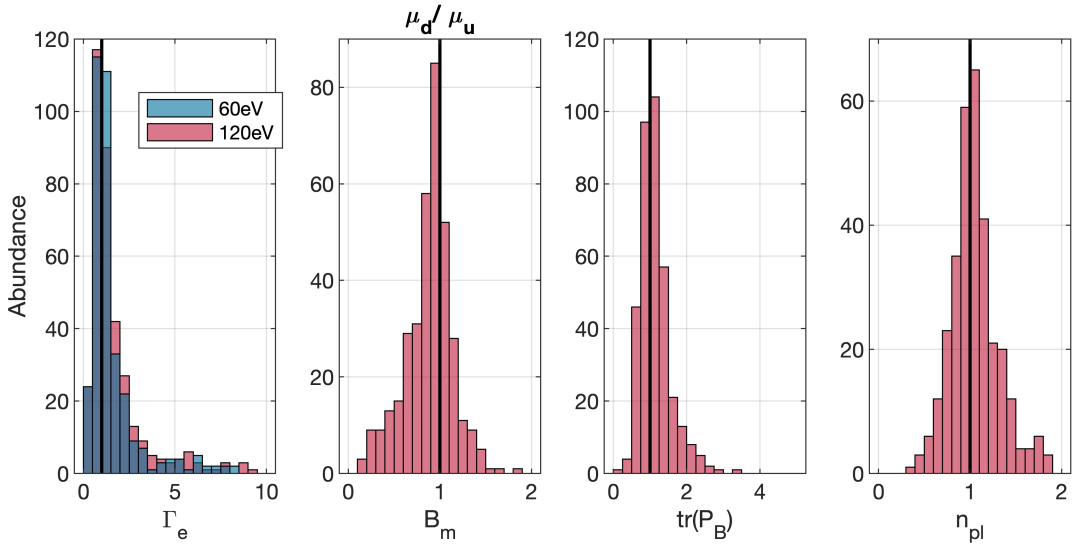

Figure 2: Comparison of the upstream and downstream mean values for ~~five~~ four of the ~~six~~ seven parameters chosen for investigation. From left to right: Electron flux Γ_e at 60 eV (blue) and at 120 eV (red), magnetic field strength B_m, trace of the magnetic field power spectral density tr(P_B), and plasma density n_{pl}.

~~in question~~are higher in the downstream region.

The parameters that we use to characterize how the plasma changes at the boundary are the proton energy H^+ E/q, the flux of the electrons $\Gamma_{IES,e}$, the magnetic field magnitude B_m, the power spectral density of the magnetic field P_B, the angle cos(θ), ~~and the spacecraft potential $V_{s/c}$~~the plasma density n_{pl}, and the proton temperature T_p. The changes are indicated in Table 1. Here, we are only looking at the qualitative changes, quantitative changes will be assessed in the next section, where the larger statistics should make up for the large uncertainty for each event. These clear, qualitative events can then be used to verify the quantitative, statistical outcome.

From these events we can conclude: Since the proton energy was used as a selection criterion the proton energy in the downstream region is always lower than upstream. The proton temperature is almost always higher in the downstream region. For the other parameters, we find that the energy of the electrons is almost always increased and the ~~spacecraft potential is often lower~~ density is often higher in the downstream region.

The statistical assessment of the proton flux is complicated by an incomplete FoV and the broad distribution of the protons. Therefore, moments of the distribution function are less representative in the situation at comet 67P. ~~Instead, we use the mean speed of the protons: a simple 1D approximation of the energy spectra of the protons. This parameter does not represent the angular spread of the particles, but it is the most representative of the energy vs. time spectrograms that we used to identify events. Even this parameter is not always reliable, as it only uses ICA spectra and some events that were identified earlier are only (better) visible in the IES spectra.~~ Therefore a direct statistical study of the moments cannot be conducted. To assess the electron flux changes, we chose two energy values (60 eV and 120 eV) to extract a 1D time series of the flux at these energies. They were chosen based on an inspection of the subset of events, ~~were~~ where these energy bands showed the clearest change.

These larger statistics agree mostly with the observations from the 13 events that were categorized by hand. From left to right:

~~$v_{m,H}$~~ ~~The proton energy (decrease) and width of the energy spectra (increase) were originally chosen as selection criteria. The downstream to upstream ratio shows a larger number of values below than above unity as expected for a decrease in energy as was seen in Sect. ??. However, the mean speed of the protons does not always decrease. This is probably due to the way that the mean speed is calculated, as it is the centre of weight of the energy spectra. For a low signal-to-noise ratio, this value is not meaningful.~~

Γ_e In our smaller subset, the energy of the electrons in the 60 eV and 120 eV band increases in 10 of the 12 inbound passes and decreases in 8 of the 12 outbound passes. In the entire dataset the electron energy is increased in the downstream region in 60% of all cases. That the larger statistics do not show the same behaviour may in part be because the energy dependent electron flux is difficult to condense to a single parameter, and the instrument sensitivity declined significantly after perihelion. We have observed cases ~~,~~where the flux was very low and thus changes were not visible.

B_m The magnetic field decreases in 68% of cases. This is consistent with the case studies above.

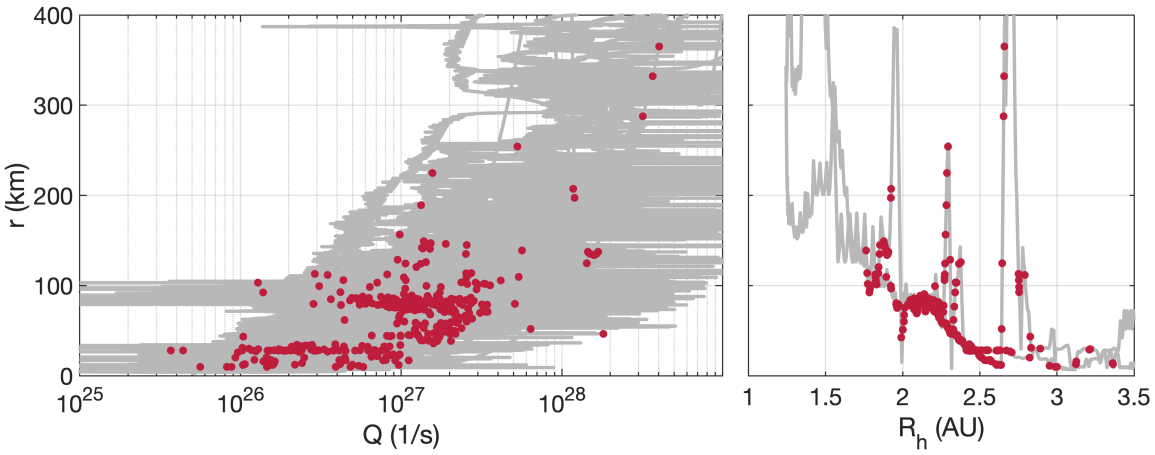

Figure 3: Cometocentric distance of the spacecraft over gas production rate (left) and heliocentric distance (right). The gas production rate was derived from measured neutral gas densities using a spherically symmetric model. The grey lines show the position during the entire Rosetta mission, while the red dots indicate boundary crossings.

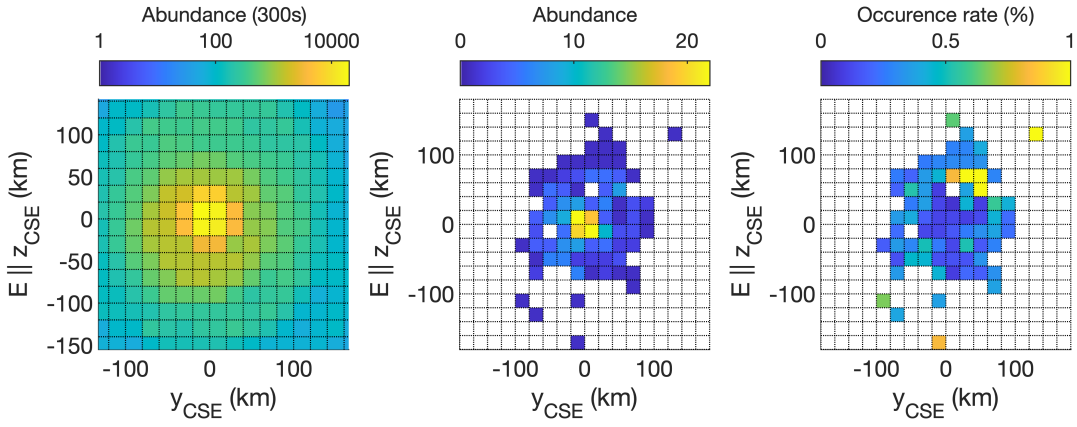

Figure 4: Abundance of the position of the spacecraft (left), position at which warm protons were detected (middle) and occurrence rate of detections normalized to the spacecraft dwell time (right). The $+E_c$ hemisphere is that of $z_{CSE} > 0$.

tr(P_B) The trace power spectral density increases downstream in 58% of all cases.

~~U_{sc}~~ ~~The spacecraft potential decreases~~

n_{pl} The plasma density increases in 52% of all cases. This is consistent with the case studies, where the ~~spacecraft potential was either decreased~~ density was either increased downstream or not changed at all.

The relevant gyroperiods of 0.5 s (protons) and 9 s (water ions) are much smaller than any of the transition times we observe. The behaviour of the magnetic field magnitude is an example of this. In shock modelling, the magnetic field is generally stronger on the downstream than the upstream side of the shock. In our statistics, we have many cases of the opposite behaviour. One possibility is that an increase in the solar wind dynamic pressure ~~pushes the~~ increases the mass-loading threshold of the plasma (Biermann et al., 1967) which means that the critical condition for a shock is met later in the flow, and thus closer to the comet. This moves the IBS further towards the ~~comet~~ nucleus and Rosetta passes into the upstream region, but at the same time the magnitude of the interplanetary field increases, resulting in a new, stronger magnetic field.

DIFdelbegin ~~When considering~~ We can also consider just the subset of events where the plasma behaves as expected for an IBS (the magnetic field increases downstream along with an increase in the power spectral density, increase in electron flux). ~~About 10% of all events fulfil all these criteria and one~~ In about 10 % of the cases all parameters that were evaluated, the magnetic field included, behave as expected at the same time. One such event is shown in Fig. ??. Although the ICA data is missing for the first half of the event (before 06:30), we can clearly see warm proton fluxes in the IES data ~~for the first half of the event. For the second half~~

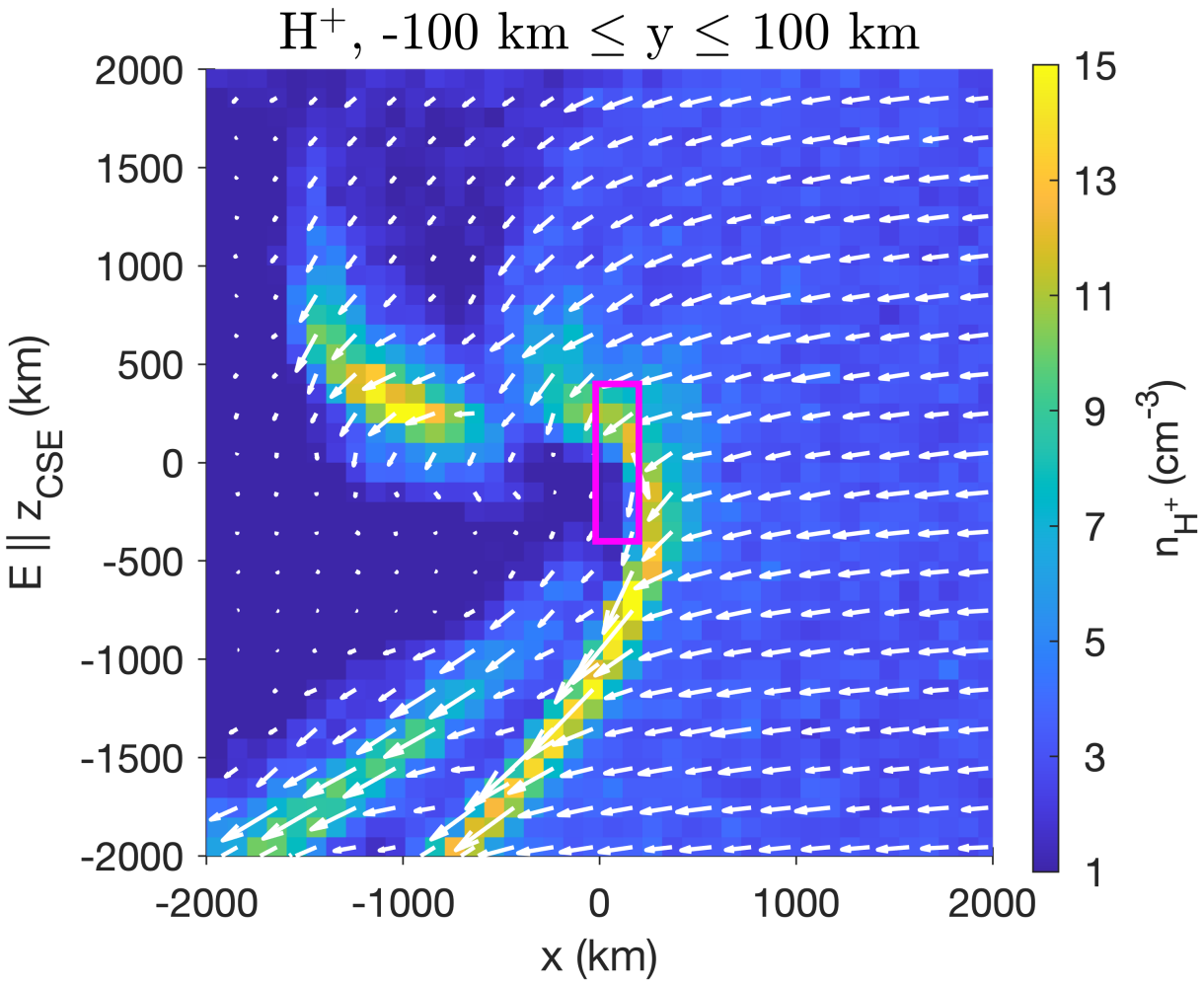

Figure 5: Density and direction of the flux of the protons from the Hybrid simulations. The simulation was run for a case of $Q = 3.2 \times 10^{27}\,s^{-1}$. For a more detailed list of parameters see Gunell et al. (2018). Here, the Sun is to the right. The IBS is roughly located where the proton density reaches its highest values (yellow).

they are registered by ICA while ICA is off. Once ICA is running, the protons do appear in the ICA energy spectra.

We present here also for the first time the spacecraft potential plasma density measurements for this boundary. We find that the spacecraft potential, and by extension the density of the plasma on average does not change significantly at the boundary. In fact, events where the plasma density increases, decreases and is unchanged can all be found in the data set. This was expected, as the plasma density at 67P at this point is dominated by the heavy ions and not the solar wind. Thus, the We can estimate the fraction of cometary ions for the event shown in Fig. 1. The cometary ion density is of the order of $1000\,\mathrm{cm}^{-3}$ and we can estimate the maximum proton density from a simple back-of-the-envelope calculation: assuming a solar wind density of $3\,\mathrm{cm}^{-3}$ (typical for heliocentric distances around 2 AU) and a compression factor of ~ 4, we get a proton density of $12\,\mathrm{cm}^{-3}$. This is close to what is also observed in the simulation used below. This gives a fraction of $\sim 99\%$ cometary ions. Even if this estimate is very rough, it is clear that the cometary ions are at this point clearly dominating the plasma density and the solar wind has only very little influence on the plasma densitydensity-wise. Instead **?** found that the solar wind and cometary ion momentum are of similar importance at the intermediate stage of cometary activity.

The gyroradii of protons in the $200 - 400\,\mathrm{km\,s}^{-1}$ range are $100 - 200\,\mathrm{km}$ in a $20\,\mathrm{nT}$ magnetic field. This is comparable to the thickness of the infant bow shock. The typical length scale of the structure in the upper left corner of Fig. 5 is about 10^3 km, corresponding to approximately 2 gyroradii in the weaker magnetic field ($\sim 10\,\mathrm{nT}$) in that region.

We have made attempts to conclusively show that this structure is indeed a shockin the fluid dynamics senseIn order to provide proof that a boundary in a plasma is a shock, usually Rankine-Hugoniot are evaluated. However, the plasma environment of the comet is far from a single fluid MHD plasma where the Rankine-Hugoniot R-H conditions could be used to investigate the transition. Such an approach has been employed in the past in the analysis of the Giotto flybys of comets 1P/Halley and 26P/Grigg–Skjellerup (Coates et al., 1990, 1997). Kessel et al. (1994) expanded the fluid theory to include effects of multiple ion species. For our situation, multi-ion and kinetic scale effectsneed to , and the non-stationarity of the shock need be accounted for.

Omidi and Winske (1987) conducted one-dimensional hybrid simulations with the aim of modelling the spacecraft encounters with comets 1P/Halley and 21P/Giacobini-Zinner. They found that for oblique interaction (cone angle 55°), shocklets form in a region of large amplitude wave activity. These shocklets convect downstream, where they break up due to dispersion, and new ones form further upstream. Thus, the process is repeated in a way that resembles shock reformation at planets (e.g. Balogh and Treumann, 2013). Although it is possible that shocklets form and shock reformation occurs also at comet 67P under certain conditions, it is not the cause of the observations reported here. The shock encounters shown in Figs. 1, **??**, 6, and 7 do not display the repetitive transitions in a wave-dominated region that would be expected for the shocklets reported by Omidi and Winske (1987).

It is may be that the infant bow shock that develops into the ordinary is the low gas production rate manifestation of what becomes the more developed cometary bow shock as the comet moves closer to the Sun and the outgassing increases furtherobserved at larger comets such as Halley.

References

André Balogh and Rudolf A. Treumann. *Physics of Collisionless Shocks*, volume 12 of *ISSI Scientific Report Series*. Springer, New York, NY, 2013. ISBN 978-1-4614-6099-2. doi: 10.1007/978-1-4614-6099-2.

E. Behar, H. Nilsson, M. Alho, C. Goetz, and B. Tsurutani. The birth and growth of a solar wind cavity around a comet - Rosetta observations. *MNRAS*, 469:S396–S403, July 2017. doi: 10.1093/mnras/stx1871.

L. Biermann, B. Brosowski, and H. U. Schmidt. The interactions of the solar wind with a comet. *Solar Physics*, 1:254–284, March 1967. doi: 10.1007/BF00150860.

A. J. Coates, A. D. Johnstone, R. L. Kessel, D. E. Huddleston, and B. Wilken. Plasma parameters near the comet Halley bow shock. *J. Geophys. Res.*, 95:20701–20716, December 1990. doi: 10.1029/JA095iA12p20701.

A. J. Coates, A. D. Johnstone, and F. M. Neubauer. Cometary ion pressure anisotropies at comets Halley and Grigg-Skjellerup. *J. Geophys. Res.*, 101(A12):27573–27584, December 1996. doi: 10.1029/96JA02524.

A. J. Coates, C. Mazelle, and F. M. Neubauer. Bow shock analysis at comets Halley and Grigg-Skjellerup. *J. Geophys. Res.*, 102(A4):7105–7113, April 1997. doi: 10.1029/96JA04002.

C. Goetz, C. Koenders, K. C. Hansen, J. Burch, C. Carr, A. Eriksson, D. Frühauff, C. Güttler, P. Henri, H. Nilsson, I. Richter, M. Rubin, H. Sierks, B. Tsurutani, M. Volwerk, and K. H. Glassmeier. Structure and evolution of the diamagnetic cavity at comet 67P/Churyumov-Gerasimenko. *MNRAS*, 462:S459–S467, November 2016a. doi: 10.1093/mnras/stw3148.

C. Goetz, C. Koenders, I. Richter, K. Altwegg, J. Burch, C. Carr, E. Cupido, A. Eriksson, C. Güttler, P. Henri, P. Mokashi, Z. Nemeth, H. Nilsson, M. Rubin, H. Sierks, B. Tsurutani, C. Vallat, M. Volwerk, and K.-H. Glassmeier. First detection of a diamagnetic cavity at comet 67P/Churyumov-Gerasimenko. *A&A*, 588:A24, April 2016b. doi: 10.1051/0004-6361/201527728.

Charlotte Götz, Herber Gunell, Martin Volwerk, Arnaud Beth, Anders Eriksson, Marina Galand, Pierre Henri, Hans Nilsson, Cyril Simon Wedlund, Markku Alho, Laila Andersson, Nicolas Andre, Johan De Keyser, Jan Deca, Yasong Ge, Karl-Heinz Glaßmeier, Rajkumar Hajra, Tomas Karlsson, Satoshi Kasahara, Ivana Kolmasova, Kristie LLera, Hadi Madanian, Ingrid Mann, Christian Mazelle, Elias Odelstad, Ferdinand Plaschke, Martin Rubin, Beatriz Sanchez-Cano, Colin Snodgrass, and Erik Vigren. Cometary Plasma Science – A White Paper in response to the Voyage 2050 Call by the European Space Agency. *arXiv e-prints*, art. arXiv:1908.00377, Aug 2019.

Herbert Gunell, Charlotte Goetz, Cyril Simon Wedlund, Jesper Lindkvist, Maria Hamrin, Hans Nilsson, Kristie Llera, Anders Eriksson, and Mats Holmström. The infant bow shock: a new frontier at a weak activity comet. *A&A*, 619:L2, November 2018. doi: 10.1051/0004-6361/201834225.

F. L. Johansson, A. I. Eriksson, N. Gilet, P. Henri, G. Wattieaux, M. G. G. T. Taylor, C. Imhof, and F. Cipriani. A charging model for the Rosetta spacecraft. *A&A*, 642:A43, October 2020. doi: 10.1051/0004-6361/202038592.

R. L. Kessel, A. J. Coates, U. Motschmann, and F. M. Neubauer. Shock normal determination for multiple-ion shocks. *J. Geophys. Res.*, 99(A10):19359–19374, October 1994. doi: 10.1029/94JA01234.

C. Koenders, K.-H. Glassmeier, I. Richter, U. Motschmann, and M. Rubin. Revisiting cometary bow shock positions. *Planetary and Space Science*, 87:85–95, October 2013. doi: 10.1016/j.pss.2013.08.009.

K. E. Mandt, A. Eriksson, N. J. T. Edberg, C. Koenders, T. Broiles, S. A. Fuselier, P. Henri, Z. Nemeth, M. Alho, N. Biver, A. Beth, J. Burch, C. Carr, K. Chae, A. J. Coates, E. Cupido, M. Galand, K.-H. Glassmeier, C. Goetz, R. Goldstein, K. C. Hansen, J. Haiducek, E. Kallio, J.-P. Lebreton, A. Luspay-Kuti, P. Mokashi, H. Nilsson, A. Opitz, I. Richter, M. Samara, K. Szego, C.-Y. Tzou, M. Volwerk, C. Simon Wedlund, and G. Stenberg Wieser. RPC observation of the development and evolution of plasma interaction boundaries at 67P/Churyumov-Gerasimenko. *MNRAS*, 462:S9–S22, November 2016. doi: 10.1093/mnras/stw1736.

F. M. Neubauer, K. H. Glassmeier, M. Pohl, J. Raeder, M. H. Acuña, L. F. Burlaga, N. F. Ness, G. Musmann, F. Mariani, M. K. Wallis, E. Ungstrup, and H. U. Schmidt. First results from the Giotto magnetometer experiment at comet Halley. *Nature*, 321:352–355, May 1986. doi: 10.1038/321352a0.

H. Nilsson, G. Stenberg Wieser, E. Behar, H. Gunell, M. Galand, C. Simon Wedlund, M. Alho, C. Goetz, M. Yamauchi, P. Henri, and E. Odelstad A.I. Eriksson. Evolution of the ion environment of comet 67P during the rosetta mission as seen by RPC-ICA. *Monthly Notices of the Royal Astronomical Society*, 469 (Suppl_2):S252–S261, 2017. doi: 10.1093/mnras/stx1491.

N. Omidi and D. Winske. A kinetic study of solar wind mass loading and cometary bow shocks. *J. Geophys. Res.*, 92(A12):13409–13426, December 1987. doi: 10.1029/JA092iA12p13409.

C. Simon Wedlund, E. Behar, H. Nilsson, M. Alho, E. Kallio, H. Gunell, D. Bodewits, K. Heritier, M. Galand, A. Beth, M. Rubin, K. Altwegg, M. Volwerk, G. Gronoff, and R. Hoekstra. Solar wind charge exchange in cometary atmospheres III. Results from the Rosetta mission to comet 67P/Churyumov-Gerasimenko. *Astronomy & Astrophysics*, 2019. doi: 10.1051/0004-6361/201834881.

Edward J. Smith, Bruce T. Tsurutani, James A. Slavin, Douglas E. Jones, George L. Siscoe, and D. Asoka Mendis. International cometary explorer encounter with Giacobini-Zinner: Magnetic field observations. *Science*, 232(4748):382–385, 1986. ISSN 0036-8075. doi: 10.1126/science.232.4748.382.

A Additional events

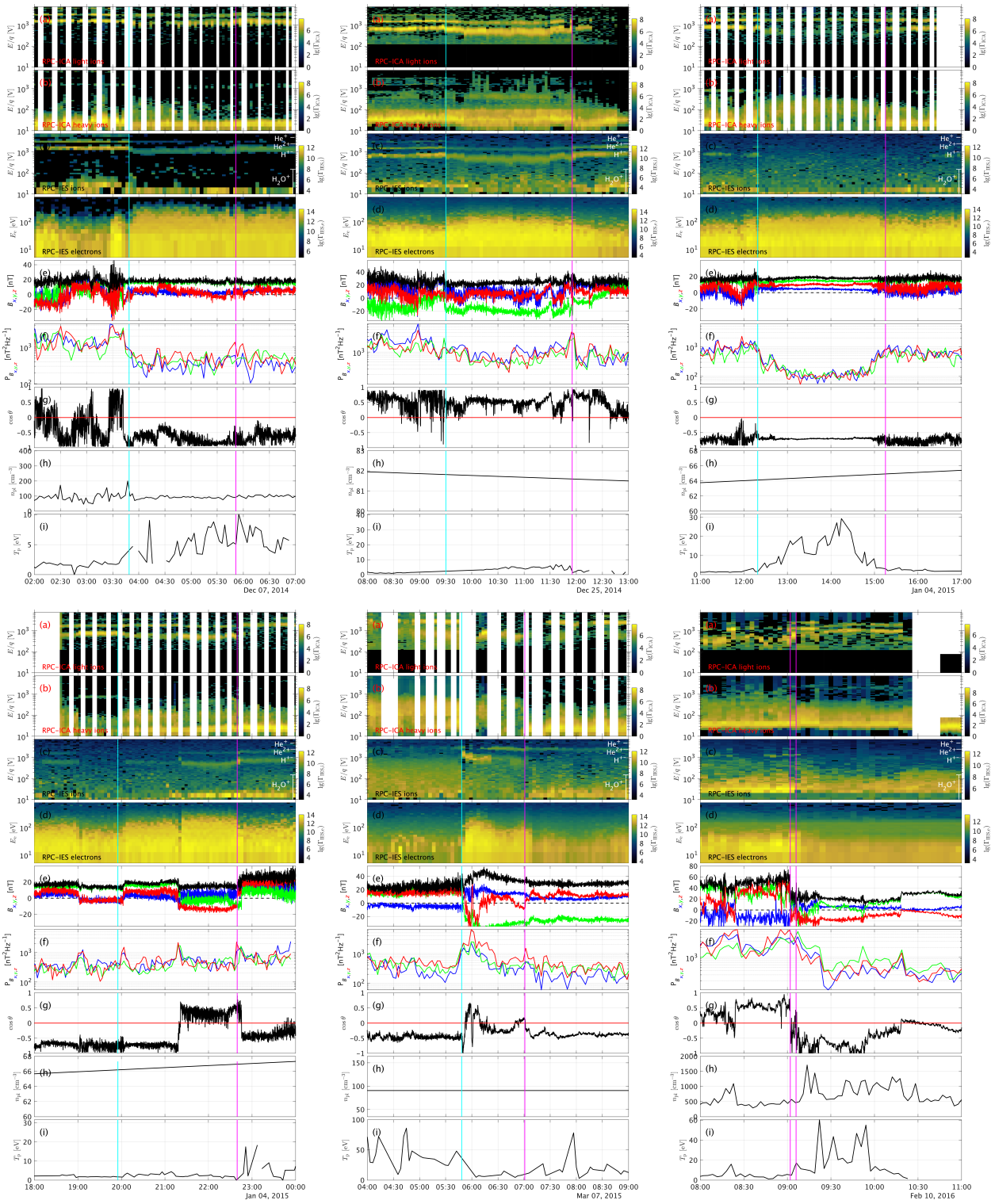

Figure 6: Observations of the plasma for the events shown in Table 1. Format is the same as in Figure 1.

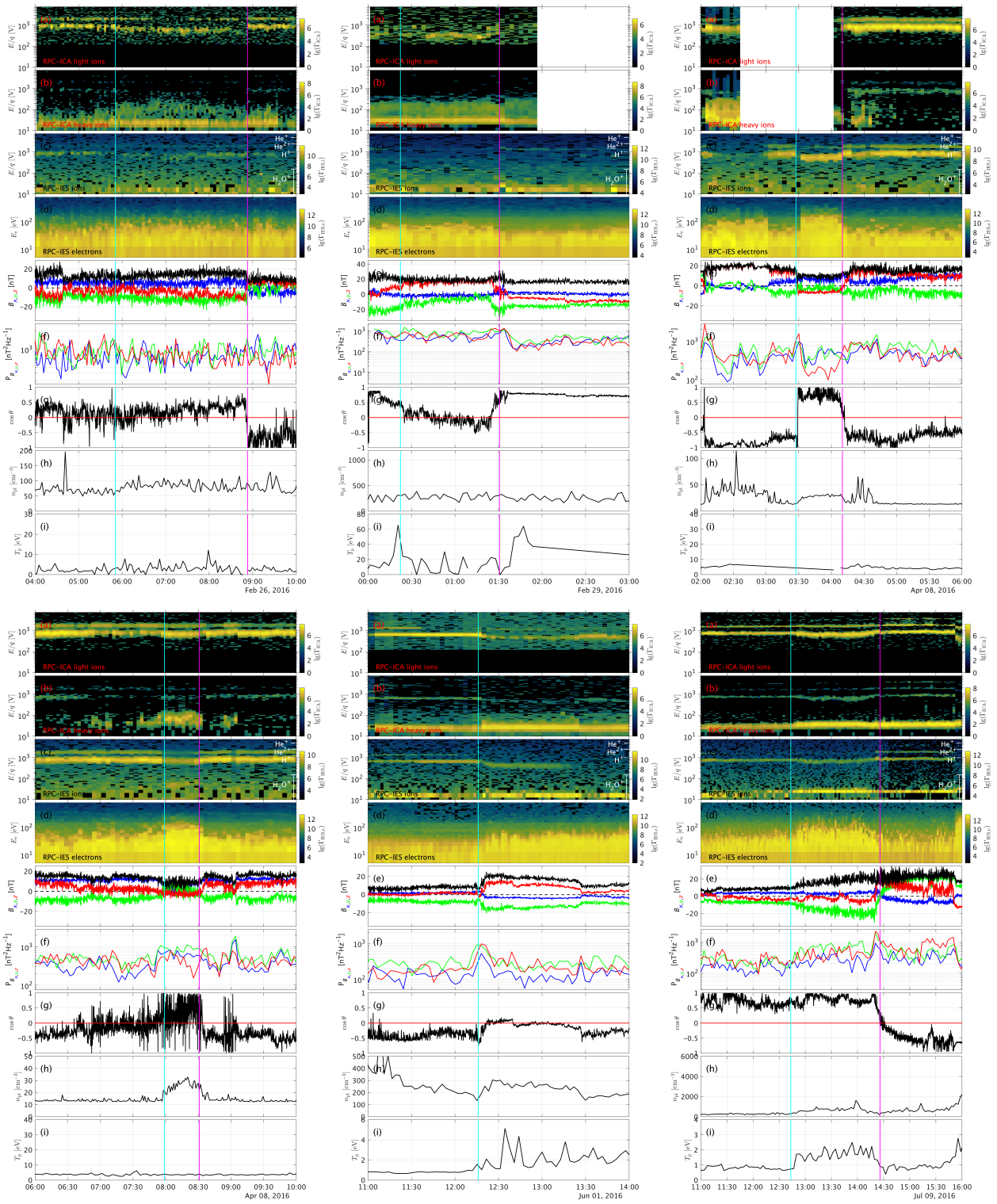

Figure 7: Observations of the plasma for the events shown in Table 1. Format is the same as in Figure 1.

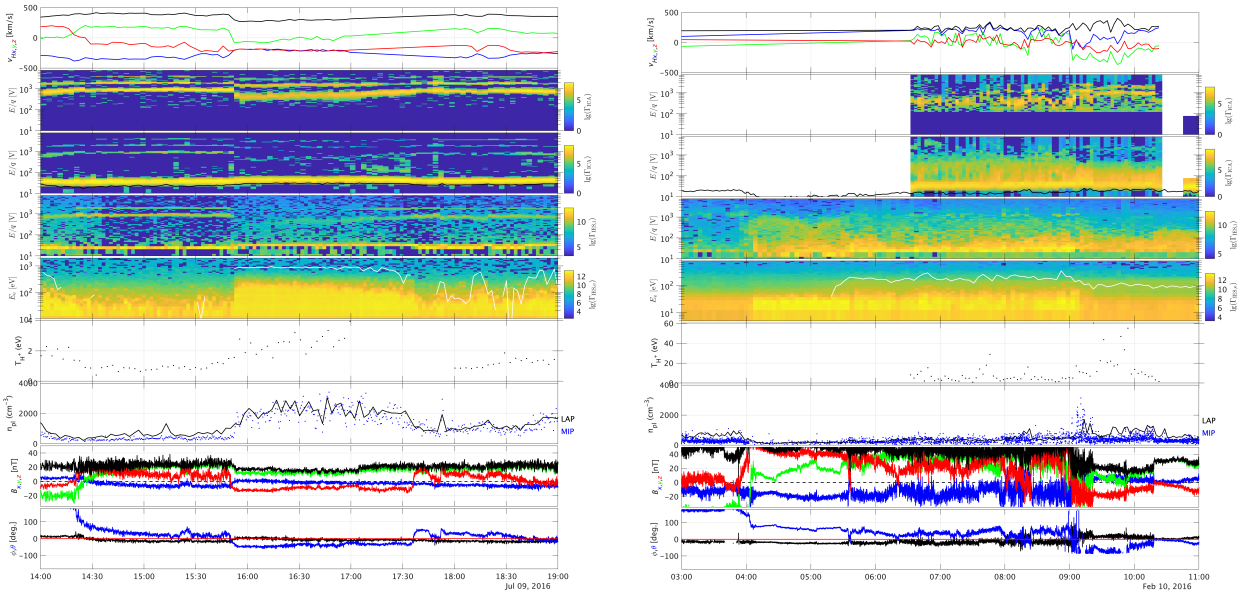

Figure 1: Left: Event from Figure 1. Right: Event from Figure 6.